Psychonomic Bulletin & Review (2022) 29:2034–2051
https://doi.org/10.3758/s13423-022-02119-8

THEORETICAL/REVIEW

A diffusion model for the congruency sequence effect

Chunming Luo[1] · **Robert W. Proctor**[2]

Accepted: 3 May 2022 / Published online: 8 June 2022
© The Psychonomic Society, Inc. 2022

Abstract
Two-choice reaction tasks for which stimuli differ on irrelevant and relevant dimensions (e.g., Simon, flanker, and Stroop tasks) show congruency effects. The diffusion model for conflict tasks (DMC) has provided a quantitative account of the mechanisms underlying decisions in such conflict tasks, but it has not been applied to the congruency sequence effect (CSE) for which the congruency on the prior trial influences performance on the current trial. The present study expands analysis of the reaction time (RT) distributions reflected by delta plots to the CSE, and then extends the DMC to simulate the results. With increasing RT: (1) the spatial Simon effect was almost unchanged following congruent trials but initially became smaller and finally reversed following incongruent trials; (2) the arrow-based Simon effects increased following both congruent and incongruent trials, but more so for the former than the latter; (3) the flanker congruency effect varied quadratically following congruent trials but increased linearly following incongruent trials. These results were modeled by the CSE-DMC, extended from the DMC with two additional assumptions: (1) feature integration influences only the controlled processes; (2) following incongruent trials, the automatic process is weakened. The results fit better with the CSE-DMC than with two variants that separately had only one of the two additional assumptions. These findings indicate that the CSEs for different conflict tasks have disparate RT distributions and that these disparities are likely due to the controlled and automatic processes being influenced differently for each trial sequence.

Keywords Diffusion model for conflict tasks · Congruency sequence effect · Simon effect · flanker effect

Introduction

Revealing the mechanisms underlying decision-making has an enduring interest for researchers in psychology, neuroscience, and economics (O'Connell et al., 2018; Ratcliff & McKoon, 2020; Ratcliff et al., 2016). Decision-making research is now endeavoring to extend models of simple decisions to more complex and ecological choice situations (Ratcliff & McKoon, 2020; Servant et al., 2015, 2016). As decision making is usually based on multiple dimensions of sensory information, decision-making models for simple choice situations have been extended to conflict tasks (e.g., Evans & Servant, 2020; Hübner et al., 2010; Janczyk & Lerche, 2019; Ulrich et al., 2015; White et al., 2011). One such model is the diffusion model for conflict tasks (DMC; Ulrich et al., 2015), which has uncovered mechanisms underlying decisions in conflict tasks such as the Simon task (Simon, 1969), flanker task (Eriksen & Eriksen, 1974), and Stroop task (Stroop, 1935/1992). The current study extends the DMC to model the congruency sequence effect (CSE) in the Simon and flanker tasks to understand the way in which the preceding trial influences the decision-making on the current trial, which is related to tradeoff between response speed and accuracy.

Reaction time (RT) distributions of Simon and flanker effects

The typical spatial Simon effect refers to an influence of the location occupied by an object on performance when people are to respond to the object or its task-relevant attributes. Simon-like effects also are obtained when people indicate the color of centered location words or single-headed

✉ Chunming Luo
luocm@psych.ac.cn

[1] CAS Key Laboratory of Behavioral Science, Institute of Psychology, 16 Lincui Road, Chaoyang District, Beijing 100101, China

[2] Department of Psychological Sciences, Purdue University, West Lafayette, IN, USA

arrows, as their spatial meanings can be processed automatically and influence responses. The various Simon effects are manifested as better performance when the task-irrelevant spatial attributes (e.g., physical locations, location words, or single-headed arrows) and correct response-positions are congruent than when they are incongruent, although left and right keypresses are arbitrarily mapped to the task-relevant non-spatial attribute (e.g., shape or color; Luo & Proctor, 2017, 2019, 2020a, 2021). The flanker effect refers to an influence on responses to a centered target of adjacent flanking distractors. Performance is better when the target and flankers signal the same response (congruent condition) than when they signal different responses (incongruent condition, Bausenhart et al., 2021; Eriksen & Eriksen, 1974; Luo & Proctor, 2016).

As reaction times (RTs) are not a normal distribution but are positively skewed, using only means to infer cognitive processes has some limitations (Ratcliff, 1979). Consequently, the RT distribution of the Simon effects is often reported along with the means in recent literature (Proctor et al., 2011; Yamaguchi & Proctor, 2012). The initial and usual method of RT distribution analysis is delta functions, also called delta plots, which present the difference of RT (or error rate or accuracy) between the incongruent and congruent conditions on the y-axis and increasing quantile bins of the RT on the x-axis (De Jong et al., 1994). The spatial Simon effect usually declines and sometimes even reverses with the increase in RT, indicating a negative or decreasing delta plot. The analysis of RT distributions also is used in studies of other conflict effects – such as the word- and arrow-based Simon effects and the flanker effect – which often increase in size as RT increases (e.g., Luo & Proctor, 2017, 2018, 2021; Ulrich et al., 2015).

The most widely accepted explanation of the various Simon effects assumes two activation processes that engage in a race. According to the race model with a dual-route concept, the Simon effects arise from activation within a direct route due to overlap of the stimuli and responses (the pre-existing associations of stimulus locations, location words or directions of arrows with response positions). The second route is an indirect one in which the activation is from the task-defined mapping of the relevant stimulus dimension to responses (the associations of relevant stimulus attribute and response position). The decreasing delta plot of the spatial Simon effect is due to the activation of the direct route occurring rapidly but then quickly dissipating, which reduces its influence the longer that responding is delayed (De Jong et al., 1994; Hommel, 1994; Luo & Proctor, 2020a; Ulrich et al., 2015). In some cases, the spatial Simon effect for slow responses even becomes negative, which is assumed to be associated with other mechanisms that suppress irrelevant response activation to prevent unwanted responses (De Jong et al., 1994; Hübner & Töbel, 2019; Ridderinkhof, 2002). For the word- or arrow-based Simon effect, the activation of the direct route intensifies gradually over time, which increases the activation's influence, generating the word- and arrow-based Simon effects as an increasing function of RT (Lu & Proctor, 2001; Luo & Proctor, 2017, 2019; Ulrich et al., 2015). The dual-route concept also has been used to explain the flanker effect and its increasing delta plot (Ulrich et al., 2015).

Diffusion model for conflict tasks (DMC)

The standard drift diffusion model for decision-making in simple two-choice tasks (Ratcliff, 1979; Ratcliff & Smith, 2004) assumes that total RT equals the duration of the decision process plus the duration of residual processes (*Ter* spent for sensory encoding and motor execution). The stimuli do not influence the residual process but the decision process $X(t)$, for which the change ($dX(t)$) in accumulated evidence for a short interval dt is determined by drift rate (μ) and a Gaussian distributed white noise ($\sigma dW(t)$). This process is formulated by the function (1):

$$dX(t) = \mu dt + \sigma dW(t) \tag{1}$$

for which $\sigma dW(t)$ is a Wiener process with mean 0 and variance $\sigma^2 dt$. The drift rate (μ) reflects the average speed with which the decision process approaches the response boundaries or threshold levels (b and $-b$). High drift rates result in faster and more accurate decisions (Pedersen et al., 2017).

The DMC (Ulrich et al., 2015) instantiated the aforementioned dual-route concepts and extended the standard drift diffusion model (Ratcliff, 1979; Ratcliff & Smith, 2004), because the standard diffusion model cannot simulate the location-based Simon effect with decreasing delta plot (Mackenzie & Dudschig, 2021; Schwarz & Miller, 2012). Different from the standard drift diffusion model where the decision process $X(t)$ is a single or unitary process, the DCM assumes that $X(t)$ is superimposed by $X_c(t)$ and $X_a(t)$, separately reflecting a controlled process and an automatic process. A correct or incorrect response is made when the superimposed process accumulates continuously over time toward one positive threshold level b (indicating selection of one response) or one negative threshold level $-b$ (indicating selection of the other response). The expected mean of $X_a(t)$ is given by function (2):

$$E\left[X_a(t)\right] = A \cdot e^{-\frac{t}{\tau}} \cdot \left[\frac{t \cdot e}{(a-1)\cdot \tau}\right]^{a-1} \tag{2}$$

where a, τ and A are shape parameter, characteristic time and peak amplitude, respectively. τ determines the time-course

of automatic activation. $\mu_a(t)$, the first derivative of $E[X_a(t)]$ with respect to t, represents the drift rate for $X_a(t)$.

$$\mu_a(t) = A \cdot e^{-\frac{t}{\tau}} \cdot \left[\frac{t \cdot e}{(a-1)\cdot\tau}\right]^{a-1} \cdot \left[\frac{a-1}{t} - \frac{1}{\tau}\right] \quad (3)$$

Let μ_c denote the drift rate of the controlled process, which is assumed to be constant. For the congruent condition, the overall drift rate is $\mu(t) = \mu_c + \mu_a(t)$, whereas for the incongruent condition, $\mu(t) = \mu_c - \mu_a(t)$. The DMC also includes a parameter z, reflecting the starting point of the accumulation process that determines whether responses are biased toward the nearest threshold.

Different from the aforementioned explanations for the shape of the delta function, the DMC posits that the shape of the delta function largely depends on how the automatic activation unfolds in time. An increasing (decreasing) delta plot means that the automatic process peaks later (earlier) in time and influences the decision for a longer (shorter) period of time. Based on this assumption, the DMC can capture conflict effects with increasing or decreasing delta plot obtained from various Simon and flanker tasks by just changing τ (Evans & Servant, 2020; Luo & Proctor, 2020a; Ulrich et al., 2015; White et al., 2018). According to the DMC, the reversal of the Simon effect occurring on slow responses could be the sign of a slight undershoot of $X_a(t)$ when it swings back to zero (Ulrich et al. 2015, p. 165). Recent electrophysiological work provided some neural data that support the proposed dynamics of the model (Servant et al., 2016).

Congruency sequence effect (CSE)

The Simon, flanker, or Stroop effect on the current trial is influenced by the preceding trial type (Egner & Hirsch, 2005; Funes et al., 2010; Gratton et al., 1992). This sequential-effect pattern is termed the conflict adaptation effect, Gratton effect, or congruency sequence effect (CSE). In those studies of CSE, a prior congruent or incongruent trial followed by the current congruent or incongruent trial form four trial sequences (cC, iC, cI, and iI, the lower-case letter indexing the preceding trial and the upper-case letter indexing the current trial). Consequently, a main and reliable finding is that the congruency effect is larger following congruent trials than following incongruent trials (e.g., Lim & Cho, 2021; Stürmer et al., 2002; Wühr & Ansorge, 2005).

The CSE was initially explained with a conflict adaptation account (Botvinick et al., 2001; Gratton et al., 1992), according to which, following an incongruent trial, attention to the distractor is decreased, resulting in a reduced congruency effect on the current trial. In contrast, following a congruent trial, attention to the distractor is sustained or increased, generating more interference from the irrelevant dimension on an incongruent current trial. Allocation of attention is assumed to result from an expectancy generated by the congruency on the preceding trial (Gratton et al., 1992) or an enhanced level of control induced by the conflict of the preceding trial (Botvinick et al., 2001; Verguts & Notebaert, 2008, 2009).

Feature integration also has been used to explain the CSE (Hommel et al., 2004; Mayr et al., 2003), based on the fact that different trial sequences have distinct feature repetitions, which may cause the differences in performance. This account is based on the theory of event coding (TEC; Hommel, 2004), which assumes that stimulus and response features are integrated within the same representational system, resulting in a binding of the stimulus and response features on a trial in an event file. This binding allows a complete match of both stimulus features from the prior trial to signal that the same response is to be made on the current trial and a complete mismatch to signal that the alternative response should be made. In contrast, partial matches of one stimulus feature but not the other do not signal whether the response should be repeated or changed and may also yield stimulus-response binding conflict (Erb et al., 2016; Hommel, 2004), slowing responses on those trials. Because complete matches/mismatches are possible only on cC and iI trial sequences, responses on those trials should be facilitated relative to those for the iC and cI trial sequences, both of which involve partial matches. Therefore, according to the feature-integration account, in a Simon or flanker task, the cC and iI trial sequences (complete match/mismatch) generate better performance than the iC and cI trial sequences (partial match), respectively, namely cC < iC and iI < cI on mean RT. When the two inequalities are summed (cC + iI < iC + cI) and cI and cC are moved left and right, respectively, the outcome is iI - iC < cI - cC, showing smaller Simon or flanker effects following incongruent trials than following congruent trials.

Both the conflict adaptation account and the feature integration account are partially supported by existing studies (for a review, see Cespón et al., 2020). The CSE was obtained in several studies with manipulations aimed to minimize integration of stimulus-response features or associative learning (Kim & Cho, 2014; Weissman et al., 2014). The CSE was also obtained, however, in studies with manipulations intended to reduce or eliminate conflict adaptation (Hommel et al., 2004; Mayr et al., 2003; Schmidt, 2013, 2019). Therefore, existing results suggest that conflict adaptation and feature integration may make separable contributions to the CSE (Spapé et al., 2011) and that both mechanisms may operate at different levels simultaneously (Abrahamse et al., 2016).

The standard diffusion model has also been used to explain the CSE. Schuch and Pütz (2021) fit the standard

diffusion model with data from parity (odd/even) and magnitude (smaller/larger than five) tasks. Results showed that the congruency effect on drift rates and on thresholds following congruent trials was larger than that following incongruent trials, indicating that differences in thresholds and drift rates between congruent and incongruent trials are reduced after experiencing response conflict. These findings agree with the idea that the experience of conflict can trigger an increase in response caution and processing selectivity, thereby attenuating the influence of task-irrelevant attributes (e.g., Erb et al., 2019; Frank, 2006; Shenhav et al., 2013).

This idea is assumed to be related to two processes underlying decision behavior: a threshold-adjustment process that increases the threshold when conflicting information is detected, and a controlled-selection process that recruits top-down resources to support goal-relevant or contextually appropriate responses (Frank, 2006; Shenhav et al., 2013). One problem for the standard diffusion model is that it cannot fit the RT distribution of the spatial Simon effect with decreasing delta plot (Schwarz & Miller, 2012; Ulrich et al., 2015), although the effect is influenced by congruency on the preceding trials. Moreover, the idea of threshold adjustment is in contrast with the assumptions by some connectionist models and diffusion models for conflict tasks, which assume that controlled and automatic processes are involved in the response decision and that threshold adjustment is not the main factor (e.g., De Pisapia & Braver, 2006; Hübner et al., 2010; Kalanthroff et al., 2018; Ulrich et al., 2015).

DMC for congruency sequence effect (CSE-DMC)

Given that the DMC can capture congruency effects with increasing or decreasing delta plots obtained from various Simon and flanker tasks by changing τ (Luo & Proctor, 2020a; Mackenzie & Dudschig, 2021; Ulrich et al., 2015), the current study examined whether a diffusion model extended from the DMC can fit the RT distributions of the CSE as reflected by delta plots. A positive conclusion would be consistent with Bausenhart et al.'s (2021) suggestion that behavioral adaptation in conflict tasks may be modeled by the DMC. In Study 1, we explored the RT distribution of the CSE using Vincentile analyses, which are reliable for the prototypical spatial Simon effect (Luo & Proctor, 2020b). Secondly, we extended the DMC to fit the cumulative distribution of CSE (we refer to this model as the CSE-DMC) and then examined whether the CSE-DMC can fit better with the data than other variants.

According to the DMC, for the congruent condition, $\mu(t) = \mu_c + \mu_a(t)$, and for the incongruent condition, $\mu(t) = \mu_c - \mu_a(t)$. For the CSE, let $\mu_{cC}(t)$, $\mu_{cI}(t)$, $\mu_{iC}(t)$, and $\mu_{iI}(t)$ denote separately the drift rates for trial sequences cC, cI, iC and iI, then $\mu_{cC}(t)$ and $\mu_{iC}(t)$ will equal μ_c plus $\mu_a(t)$, and $\mu_{cI}(t)$, and $\mu_{iI}(t)$ will equal μ_c minus $\mu_a(t)$, if there are no effects of preceding trials on the current trials. Given that the CSE is reliable, the DMC might not fit well with the data for the CSE and need some extensions. Therefore, besides following the assumptions of the DMC that the controlled and automatic processes accumulate differently and independently, the CSE-DMC added two other assumptions inspired by the conflict adaptation and feature integration accounts and the findings with the standard diffusion model. These two assumptions were added because, as noted, existing results suggest that conflict adaptation and feature integration may make separable contributions to the CSE (Spapé et al., 2011) and that both mechanisms may operate at different levels simultaneously (Abrahamse et al., 2016; Cespón et al., 2020).

First, we assumed that feature integration influences only the controlled processes. Although the feature integration account does not explicitly distinguish controlled and automatic processes, it is reasonable to attribute that component to controlled processes because (1) the integrated event file is a short-term memory code (Hommel & Frings, 2020) and (2) "same response if complete match and alternative response if complete mismatch" is a strategic rule consistent with the instructed goal of responding as fast as possible (Hommel, 2022). As complete repetition or switch of trial type speeds up the responses for cC and iI trial sequences, although in different degrees, we used only one parameter μ_{cL} for the controlled processes for cC and iI trial sequences. Because partial repetition may slow down the responses for cI and iC trial sequences due to stimulus-response binding conflict, we used one parameter μ_c for iC and cI trial sequences. μ_c is smaller than μ_{cL}. This assumption is consistent with the idea that a controlled selection process likely recruits top-down resources to support goal-relevant or contextually appropriate responses (De Pisapia & Braver, 2006; Erb et al., 2016; Hübner et al., 2010; Frank, 2006; Kalanthroff et al., 2018; Shenhav et al., 2013 Ulrich et al., 2015). In connectionist models, a similar mechanism is called proactive control (De Pisapia & Braver, 2006; Kalanthroff et al., 2018).

Second, we assumed that following incongruent trials the automatic processes are influenced, resulting in more attention being paid to the task-relevant attribute (or target) and less to the task-irrelevant attribute (or distractor), reducing its influence. This assumption is inspired by the conflict-adaptation account, but it does not consider that this influence is exerted by way of the controlled process. As Hommel et al. (2004) noted, "that the magnitude of the Simon effect varies as a function of the correspondence relation of the previous trial does not necessarily indicate that the unconditional, or automatic, route is under voluntary control" (pp. 2–3). Our assumption is compatible with some connectionist

and diffusion models for conflict tasks, which assume that automatic activation by irrelevant stimulus information is involved in the response decision (e.g., Bausenhart et al., 2021; De Pisapia & Braver, 2006; Hübner et al., 2010; Kalanthroff et al., 2018; Ulrich et al., 2015). In connectionist models, a similar mechanism is called reactive control (De Pisapia & Braver, 2006; Kalanthroff et al., 2018).

According to this automatic-process assumption, for iC and iI trial sequences, $\mu_a(t)$ for the automatic processes becomes smaller, and we used $\mu_{aS}(t)$ to specify the processes, as shown in function (4). As $\mu_a(t)$ is represented by function (3), it includes a usually fixed parameter $a = 2$ and two possible changing parameters A and τ, for which we used A_S and τs to represent the latter two parameters for iC and iI trial sequences.

$$\mu_{aS}(t) = A_S \cdot e^{-\frac{t}{\tau s}} \cdot \left[\frac{t \cdot e}{(a-1)\cdot \tau s}\right]^{a-1} \cdot \left[\frac{a-1}{t} - \frac{1}{\tau s}\right] \quad (4)$$

Thus, as shown in Table 1, for cC trials, $\mu_{cC}(t) = \mu_{cL} + \mu_a(t)$, and for iI trials, $\mu_{iI}(t) = \mu_{cL} - \mu_{aS}(t)$, whereas for cI and iC trial conditions, $\mu_{cI}(t) = \mu_c - \mu_a(t)$ and $\mu_{iC}(t) = \mu_c + \mu_{aS}(t)$. For the CSE-DMC, except for the drift rates, b and the other parameters are identical across trial sequences, so the RT and accuracy for each trial sequence are determined by their corresponding drift rate. Consequently, the Simon effect following congruent trials is determined by the difference between $\mu_{cC}(t)$ and $\mu_{cI}(t)$, whereas the Simon effect following incongruent trials is determined by the difference between $\mu_{iC}(t)$ and $\mu_{iI}(t)$. Because $\mu_{cC}(t) - \mu_{cI}(t)$ equals $\mu_{cL} - \mu_c + 2\mu_a(t)$, which is larger than $\mu_{iC}(t) - \mu_{iI}(t)$ that equals $\mu_c - \mu_{cL} + 2\mu_{aS}(t)$, the CSE-DMC model predicts a larger Simon effect following congruent trials than following incongruent trials. Moreover, for the CSE-DMC, we can get $\mu_{cI}(t) < \mu_{iC}(t) < \mu_{cC}(t)$ and $\mu_{cI}(t) < \mu_{iI}(t) < \mu_{cC}(t)$, but $\mu_{iI}(t)$ minus $\mu_{iC}(t)$ equals $\mu_{cL} - \mu_c - 2\mu_{aS}(t)$, which determines the difference between $\mu_{iI}(t)$ and $\mu_{iC}(t)$. According to function (1), when the threshold and other parameters are constant across trial sequences, the size of drift rate for each trial sequence determines the decisions related to the tradeoff between response speed and accuracy, with high drift rates resulting in faster and more accurate decisions (Pedersen et al., 2017).

In addition to the CSE-DMC model, we also fit the data to an alternative model that only has the aforementioned first assumption and another alternative model that only has the second assumption. We refer to the alternative models as FI-DMC and CA-DMC, respectively. In the FI-DMC, for cC trials, $\mu_{cC}(t) = \mu_{cL} + \mu_a(t)$, and for iI trials, $\mu_{iI}(t) = \mu_{cL} - \mu_a(t)$, whereas for cI and iC trial conditions, $\mu_{cI}(t) = \mu_c - \mu_a(t)$ and $\mu_{iC}(t) = \mu_c + \mu_a(t)$. In the CA-DMC, for cC trials, $\mu_{cC}(t) = \mu_c + \mu_a(t)$, and for iI trials, $\mu_{iI}(t) = \mu_c - \mu_{aS}(t)$, whereas for cI and iC trial conditions, $\mu_{cI}(t) = \mu_c - \mu_a(t)$ and $\mu_{iC}(t) = \mu_c + \mu_{aS}(t)$.

In Studies 2 and 3, we evaluated whether the CSE-DMC also can fit the cumulative distributions of the CSE for the arrow-based Simon effect and flanker effect with increasing delta plots. The purpose of doing so was to examine whether the CSE-DMC can be extended to simulate other conflict effects with increasing delta plots. To our knowledge, few studies have addressed the issue of whether and how the preceding trials influence decision-making in the current trials with a model-based approach. Addressing this issue can further understanding about how complex task contexts influence decisions.

Table 1 Mean accuracy (%) and reaction time (RT, in ms) with standard deviations in parentheses and number of trials (NT), for cC, cI, iC and iI Trial sequences in Studys 1 to 3. $\mu_a(t)$ and μ_c for the automatic and the controlled processes, and μ_{cL} for the automatic processes enhanced by trial repetition, and $\mu_{aS}(t)$ for controlled processes reduced by previous trial

	Trial sequence	Drift rate (μ)	NT	Accuracy	RT
Study 1	cC	$\mu_{cL} + \mu_a(t)$	62	99.0(1.4)	443(85)
	cI	$\mu_c - \mu_a(t)$	61	95.3(4.9)	487(91)
	iC	$\mu_c + \mu_{aS}(t)$	61	96.2(3.7)	472(85)
	iI	$\mu_{cL} - \mu_{aS}(t)$	61	96.4(2.6)	477(86)
Study 2	cC	$\mu_{cL} + \mu_a(t)$	61	98.8(1.7)	404(47)
	cI	$\mu_c - \mu_a(t)$	61	95.4(4.6)	442(55)
	iC	$\mu_c + \mu_{aS}(t)$	60	98.8(1.3)	410(49)
	iI	$\mu_{cL} - \mu_{aS}(t)$	60	97.8(2.4)	424(55)
Study 3	cC	$\mu_{cL} + \mu_{a(t)}$	60	94.2(3.8)	441(21)
	cI	$\mu_c - \mu_{a(t)}$	61	93.1(3.8)	468(24)
	iC	$\mu_c + \mu_{aS(t)}$	62	94.2(3.8)	446(22)
	iI	$\mu_{cL} - \mu_{aS(t)}$	61	92.9(3.7)	465(24)

Study 1: RT distributions of CSE and model comparison for spatial Simon task

We analyzed and modeled the data from Experiment 1A in Luo and Proctor (2019), where 20 participants indicated the color of a square that was presented 4.8° to the left or right of the center of a display screen. Each participant performed two blocks of 128 trials. Luo and Proctor (2019) focused on the Simon effect that served as a baseline, but they did not investigate the effects of preceding trials on the Simon effects obtained on the upcoming trials. RT distribution analysis showed that the location-based Simon effect decreased linearly from bin 1 to bin 5 (39, 31, 24, 18, and 7 ms, respectively), indicating a negative-going delta plot.

In the current Study 1, we first analyzed the CSE by using Vincentile analysis, as in Luo and Proctor (2019), to analyze the RT distributions for CSE. Then, based on the RT distributions, we fit them with the CSE-DMC to examine whether

it can fit the data well and better than that of the two variants, the FI-DMC and CA-DMC models.

Method

We coded the trial sequences: a congruent trial followed by another congruent one (cC) and by an incongruent trial (cI); an incongruent trial followed by a congruent (iC) trial and by an incongruent trial (iI). The first trial in each block and the trial following a trial with an error response or non-response, were excluded in the accuracy analysis. The data for accuracy analysis were then analyzed as follows. RTs for responses (including error and correct responses) for each block were rank ordered from shortest to longest for each trial sequence for each participant, and divided into five equally sized bins. Then, mean accuracy of each bin per trial sequence for each participant across blocks was calculated, generating the conditional accuracy function (CAF). Lastly, a repeated-measures analysis of variance (ANOVA) was performed on accuracy, with bin, preceding congruency, and current congruency as within-subject variables.

In the RT data analysis, we excluded test trials wherein participants responded incorrectly to the target and test trials with RTs beyond 3 standard deviations (SDs) of the mean for each trial sequence for each participant. The means for the remaining RTs for each trial sequence are presented in Table 1. Those remaining RTs were rank ordered from shortest to longest for each trial sequence for each participant; percentiles (10, 30, 50, 70, 90%) of correct RTs were estimated for each participant and each trial sequence, generating the conditional duration function (CDF). The mean RTs for each trial sequence and the Simon effects were then calculated for each percentile. A repeated-measures ANOVA was performed on RT, with percentile, preceding congruency, and current congruency as within-subject variables. Considering the way in which the RT data were grouped, the percentile main effect on RT was invariably significant, so it is not reported and discussed.

The model fitting procedure was similar to the method described by Hübner (2014), Servant et al. (2016), and Mahani et al. (2019). Each Model was fitted separately to the CAFs and the CDFs for each of the four conditions (cC, cI, iC, iI). There were five CAF bins (0–20%, 20%–40%, 40%–60%, 60%–80%, and 80%–100%), and five CDF quantiles (0.10, 0.30, 0.50, 0.70, and 0.90) for each condition. Predictions of each model were generated using Monte Carlo simulations (Metropolis & Ulam, 1949) with a step size of $\Delta t = 1$ ms, and a diffusion constant of $\sigma = 4$ for the superimposed process and a (the shape parameter of the scaled gamma function of the automatic process for stimulus location) equals 2. The following equation (5) was used to fit each model to the data:

$$G^2 = 2\sum_{i=1}^{4} N_i \sum_{j=1}^{10} \mid P_{ij} \log \frac{P_{ij}}{Q_{ij}} \mid \tag{5}$$

where P_{ij} and Q_{ij} denote the observed and the predicted proportion of responses, respectively, and N_i is the number of trials per condition. The index i indicates the trial sequence, and the summation over the j includes both CAFs (five bins) and CDFs (five bins). 100,000 trials were simulated for each condition and minimization cycle. The G^2 criterion was minimized with the MATLAB implementation of the Nelder–Mead SIMPLEX method (Lagarias et al., 1998). As SIMPLEX is sensitive to the initial parameter values, the fitting procedure was repeated with 20 different sets of initial values, each set being a random draw from the uniform distributions defined in Table 2; the lower and upper bounds are from prior studies (Evans & Servant, 2020; Luo & Proctor, 2020a; White et al., 2018). Model selection for the CSE was made by computing a *BIC* statistic that penalizes models according to their number of free parameters f:

$$BIC = G^2 + f \log \sum_{i=1}^{4} N_i \tag{6}$$

Results

Vincentile analysis on accuracy

The numbers of trials for each trial sequence across participants are shown in Table 1. The main effect of preceding congruency was not significant, but that of bin was, and the main effect of current congruency yielded probability < .10, $F(1, 19) = 2.42$, $p = .136$, $MSE = .003$, $\eta_p^2 = .113$; $F(4, 76) = 7.50$, $p < .001$, $MSE = .004$, $\eta_p^2 = .283$; $F(1, 19) = 3.45$, $p = .079$, $MSE = .009$, $\eta_p^2 = .154$. The preceding congruency × current congruency interaction was significant, $F(1, 19) = 11.80$, $p = .003$, $MSE = .003$, $\eta_p^2 = .383$: The Simon effect was larger following congruent trials (3.68%) than following incongruent trials (-0.18%).

The two-way interactions between preceding congruency and bin, and between current congruency and bin, were significant, $F(4, 76) = 5.01$, $p < .001$, $MSE = .004$, $\eta_p^2 = .209$; $F(4, 76) = 10.90$, $p < .001$, $MSE = .004$, $\eta_p^2 = .364$, as was the three-way interaction of preceding congruency × current congruency × bin, $F(4, 76) = 2.98$, $p = .024$, MSE = .003, $\eta_p^2 = .136$. Trend analysis showed that following a congruent trial, the Simon effect (CI - CC) change from bin 1 to bin 5 had linear, quadratic, and cubic components, $Fs(1, 19) = 12.32$, 12.50, and 26,60, $ps = .002$, and < .001, $MSEs = .014$, .008, and .002, $\eta_p^2 = .393$, .397, and .583, respectively, indicating a negative-going delta plot (see Fig. 1). Following an incongruent trial, the Simon effect (II - IC) changed quadratically from bin 1 to bin 5, $F(1, 19) = 8.91$, $p = .008$, $MSE = .011$, $\eta_p^2 = .319$, also indicating a negative-going delta

Table 2 Parameter estimates of the CSE-DMC, FI-DMC, and CA-DMC for the CSE in Studies 1, 2, and 3. LB (lower bound) and UB (upper bound) are used to constrain parameter space of the three models

		Parameters									
		b	μ_c	μ_R	σ_R	A	τ	σ_z	μ_{cL}	A_s	τ_s
	LB	51	.20	240	26	5	20	5	.20	5	20
	UB	70	.80	359	47	25	332	19	.80	25	332
Study 1	CSE-DMC	68	.45	334	47	21	35	18	.49	16	22
	FI-DMC	70	.43	326	35	13	46	12	.50		
	CA-DMC	69	.45	324	35	15	66	11		6	32
Study 2	CSE-DMC	65	.53	303	37	18	331	11	.56	7	296
	FI-DMC	63	.54	312	40	14	317	7	.61		
	CA-DMC	67	.53	299	33	16	331	10		6	320
Study 3	CSE-DMC	68	.52	351	34	10	77	13	.55	7	120
	FI-DMC	67	.52	350	28	8	78	8	.54		
	CA-DMC	70	.53	345	30	10	90	16		10	324

The parameters are b (decision boundary), μ_c and μ_{cL} (drift rate of the controlled process), μ_R (duration of all non-decisional processes), σ_R (variability of the duration of non-decisional processes), A and A_s (amplitude of the automatic process), τ and τ_s (the time-course of automatic activation, and σ_z (starting point variability of the superimposed accumulation process)

DMC diffusion model for conflict tasks, *CSE* congruency sequence effect

plot (see Fig. 1). These results show that the Simon effects on accuracy following congruent trials or incongruent trials became smaller across the RT distribution as RT increased.

Vincentile analysis on RT

Mean RT and standard deviation SD per trial sequence across participants are shown in Table 1. The main effects of preceding congruency, current congruency, and bin were significant, $F(1, 19) = 5.96$, $p = .025$, $MSE = 1{,}292$, $\eta_p^2 = .239$; $F(1, 19) = 24.86$, $p < .001$, $MSE = 2{,}513$, $\eta_p^2 = .567$; $F(4, 76) = 154.47$, $p < .001$, $MSE = 4{,}812$, $\eta_p^2 = .890$. There was also an interaction between preceding congruency and current congruency, $F(1, 19) = 40.22$, $p < .001$, $MSE = 980$, $\eta_p^2 = .679$, indicating that the Simon effect was larger following congruent trials (44 ms) than following incongruent trials (5 ms).

The two-way interactions of preceding congruency × bin and of current congruency × bin were not significant, $F(4, 76) = 1.03$, $p = .397$, $MSE = 440$, $\eta_p^2 = .051$; $F(4, 76) = 2.22$, $p = .075$, $MSE = 821$, $\eta_p^2 = .104$, but the three-way interaction of preceding congruency × current congruency × bin was, $F(4, 76) = 2.85$, $p = .030$, $MSE = 269$, $\eta_p^2 = .130$. When the preceding trial was congruent, trend analysis showed that the Simon effect (CI - CC) did not change significantly from bin 1 to bin 5 (55, 45, 44, 46, and 39 ms, respectively), $F < 1$ (see Fig. 1). Following an incongruent trial, the Simon effect (II - IC) decreased linearly from bin 1 to bin 5 (26, 15, 4, -5, and -13 ms, respectively), $F(1, 19) = 10.56$, $p = .004$, $MSE = 1{,}812$, $\eta_p^2 = .357$, indicating a negative-going delta plot (see Fig. 1). These results show that the Simon effects following congruent and incongruent trials had different RT distributions, as the former did not change significantly as RT increased, whereas the latter decreased.

Model fitting and comparison

The fits of the FI-DMC, CA-DMC and CSE-DMC models were compared by using the paired-sample permutation test across 1,000 simulated G^2 and *BIC* values with 100,000 permutations. The FI-DMC and CA-DMC had larger G^2 (68.7 and 57.5) and *BIC* (112.7 and 107.0) values compared with the CSE-DMC ($G^2 = 47.6$; $BIC = 102.6$), $ps < .001$. Results for the CSE together with predictions by the FI-DMC and CA-DMC and CSE-DMC models are shown in Fig. 1. The parameters of the FI-DMC, CA-DMC and CSE-DMC models are shown in Table 2. These results indicate that the CSE-DMC could fit the data well and provided a better fit with the data than the other models.

Discussion

On mean RT, the Simon effect was larger following congruent trials than following incongruent trials, replicating previous findings (Funes et al., 2010; Hommel et al., 2004; Kerns, 2006; Stürmer et al., 2002; Wühr & Ansorge, 2005). Somewhat different from most prior studies, which primarily focused on the mean RT (but see Ridderinkhof, 2002;

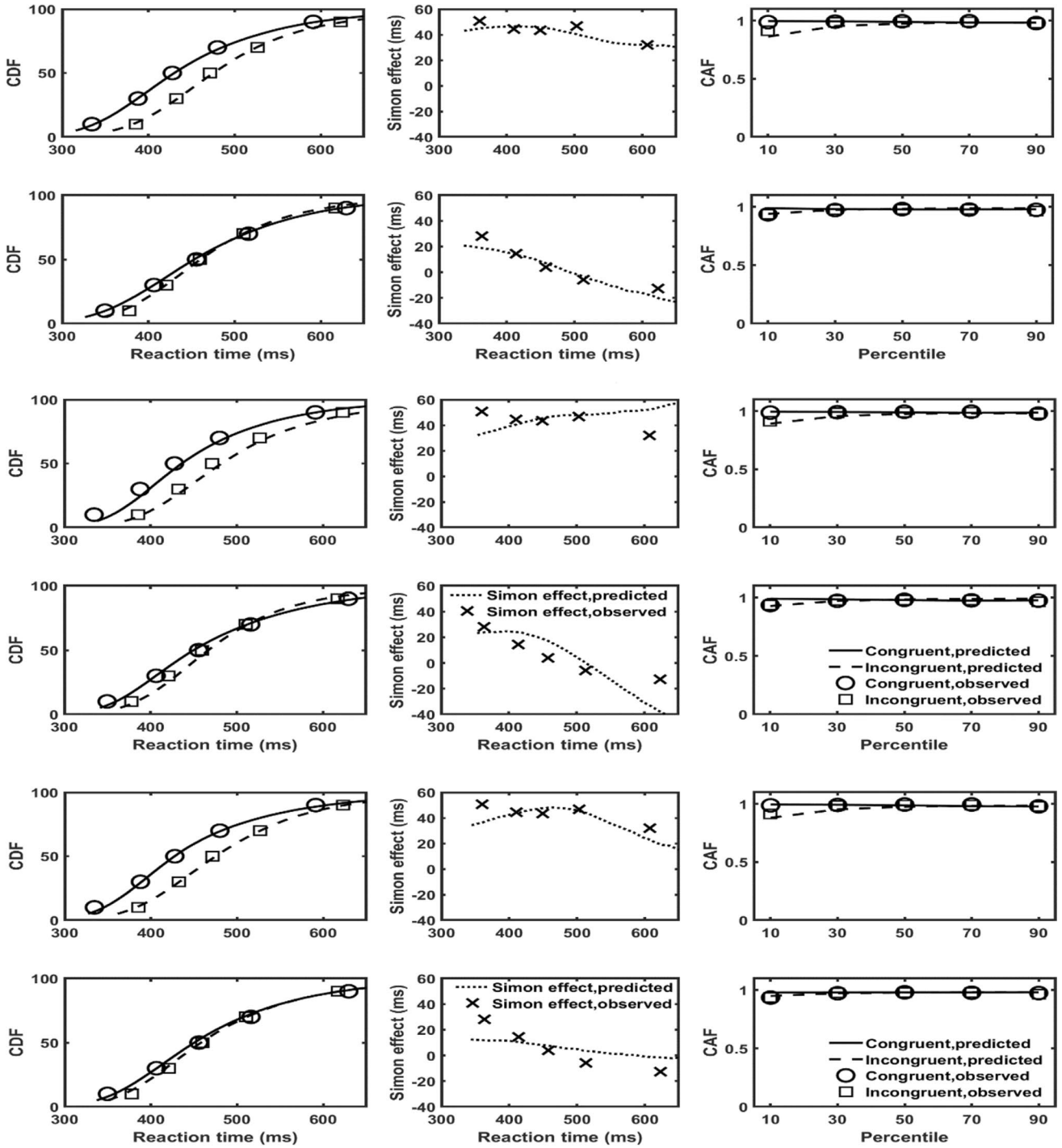

Fig. 1 Conditional duration functions, delta plots and conditional accuracy functions (circles, squares and crosses) for the CSE in Study 1, together with predictions (solid, dashed and dotted lines) by the CSE-DMC, FI-DMC and CA-DMC. The first two rows for the CSE-DMC, the third and fourth for the FI-DMC, and the fifth and sixth for the CA-DMC. The first, third, and fifth rows for congruent and congruent trials following congruent trials, and the others for congruent and incongruent trials following incongruent trials. *DMC* = diffusion model for conflict tasks, *CSE* = congruency sequence effect

Töbel et al., 2014, for exceptions), we also analyzed the mean accuracy. The results of the accuracy analysis were parallel with the results for mean RT.

Notably, the Simon effect on accuracy decreased with the increase of RT, invariant of whether the prior trial was congruent or incongruent, showing a negative-going delta plot.

On mean RT, following congruent trials, the Simon effect was almost unchanged with the increase of RT, whereas following incongruent trials, the Simon effect became smaller with increasing RT, showing a negative-going delta plot. These results are similar to those shown in Fig. 2 of Töbel et al. (2014), although they did not test separately the changes of Simon effect with increasing RT following congruent and incongruent trials. The current results, together with those of Töbel et al. (2014), showed that the spatial Simon effects on mean accuracy, RT, and RT distribution were influenced by the congruency of prior trial. Model fitting and comparison showed that the CSE-DMC could fit the CSE well, and it provided a better fit than the other variants.

Study 2: RT distributions of CSE and model comparison for arrow-based Simon task

We analyzed and modeled the data from Experiment 1C in Luo and Proctor (2019), where 20 participants indicated the color of a left- or right-pointing arrow presented on the center of a display screen. Each participant performed two blocks of 128 trials. Luo and Proctor (2019) focused on the arrow-based Simon effect that served as a baseline, but they did not investigate the effects of preceding trials on the Simon effects obtained on the current trials. The results showed that the arrow-based Simon effect on RT increased linearly from bin 1 to bin 5 (6, 14, 26, 40, and 60 ms, respectively), indicating a positive-going delta plot.

In the current study 2, we first used Vincentile analysis, as in Luo and Proctor (2019), to analyze the RT distributions for CSE. Then, based on the RT distributions, we fit them with the CSE-DMC to examine whether it can fit the data well and whether the fit is better than that of two other variants, the FI-DMC and the CA-DMC model. This study was to understand whether the CSE-DMC can summarize the results from arrow-based Simon task, which differ from those of the location-based task, and whether the fit is better than that of two other model variants.

Method

The trial sequences were coded as in Study 1: cC, cI, iC, and iI, with the letters standing for preceding congruency (c and i) and current congruency (C and I). CAFs and CDFs were calculated as in Study 1, and the ANOVAs on them and the model fitting procedure were identical to those in Study 1.

Results

Vincentile analysis on accuracy

The numbers of trials for each trial sequence across participants are shown in Table 1. The main effects of preceding congruency, current congruency, and bin were significant, $F(1, 19) = 8.22$, $p = .010$, $MSE = .002$, $\eta_p^2 = .302$; $F(1, 19) = 11.88$, $p = .003$, $MSE = .004$, $\eta_p^2 = .385$; $F(4, 76) = 2.98$, $p = .024$, $MSE = .003$, $\eta_p^2 = .135$. The preceding congruency × current congruency interaction approached significance, $F(1, 19) = 4.30$, $p = .052$, $MSE = .003$, $\eta_p^2 = .185$, with the Simon effect tending to be larger following congruent trials (3.45%) than following incongruent trials (1.06%).

The two-way interactions between preceding congruency and bin, and between current congruency and bin, and the three-way interaction between preceding congruency, current congruency and bin were not significant, $F(4, 76) = 1.26$, $p = .295$, $MSE = .002$, $\eta_p^2 = .062$; $F(4, 76) = 2.01$, $p = .10$, $MSE = .002$, $\eta_p^2 = .096$; $F < 1$.

Vincentile analysis on RT

Mean RT and SD per trial sequence across participants are shown in Table 1. The main effects of preceding congruency, current congruency, and bin were significant, $F(1, 19) = 6.39$, $p = .020$, $MSE = 527$, $\eta_p^2 = .252$; $F(1, 19) = 47.18$, $p < .001$, $MSE = 1{,}401$, $\eta_p^2 = .713$; $F(4, 76) = 148.15$, $p < .001$, $MSE = 3{,}383$, $\eta_p^2 = .886$. Preceding congruency interacted with current congruency, $F(1, 19) = 19.49$, $p < .001$, $MSE = 683$, $\eta_p^2 = .506$, with the Simon effect being larger following congruent trials (37 ms) than following incongruent trials (14 ms).

The two-way interactions of preceding congruency × bin and of current congruency × bin were significant, $F(4, 76) = 3.57$, $p = .010$, $MSE = 182$, $\eta_p^2 = .158$; $F(4, 76) = 15.53$, $p < .001$, $MSE = 384$, $\eta_p^2 = .450$, as well as the three-way interaction of preceding congruency × current congruency × bin, $F(4, 76) = 2.64$, $p = .040$, $MSE = 187$, $\eta_p^2 = .122$. When the preceding trial was congruent, trend analysis showed that the Simon effect (cI - cC) increased linearly from bin 1 to bin 5 (12, 21, 36, 52 and 66 ms, respectively), $F(1, 19) = 27.67$, $p < .001$, $MSE = 1{,}380$, $\eta_p^2 = .593$ (see Figure 2), indicating a positive-going delta plot. Following an incongruent trial, the Simon effect (iI - iC) also increased linearly from bin 1 to bin 5 (-4, 7, 17, 22 and 29 ms, respectively), $F(1, 19) = 13.42$, $p = .002$, $MSE = 956$, $\eta_p^2 = .414$, also indicating a positive-going delta plot (see Fig. 2). These results show that the Simon effects following congruent and incongruent trials had somewhat different RT distributions: the former increased more rapidly than the latter as RT increased.

Model fitting and comparison

The fits of the FI-DMC, CA-DMC and CSE-DMC models were compared using the paired-sample permutation test across 1,000 simulated G^2 and *BIC* values with 100,000 permutations. The FI-DMC and CA-DMC had larger G^2 (47.7

and 49.2) and *BIC* (103.8 and 99.1) values compared with the CSE-DMC ($G^2 = 39.9$; $BIC = 94.4$), $ps < .001$. Results for the CSE together with predictions by the FI-DMC and CA-DMC and CSE-DMC models are shown in Fig. 2. The parameters of the FI-DMC, CA-DMC and CSE-DMC models are shown in Table 2. These results indicate that the CSE-DMC could fit the data well and that it provided a better fit with the data than the other models.

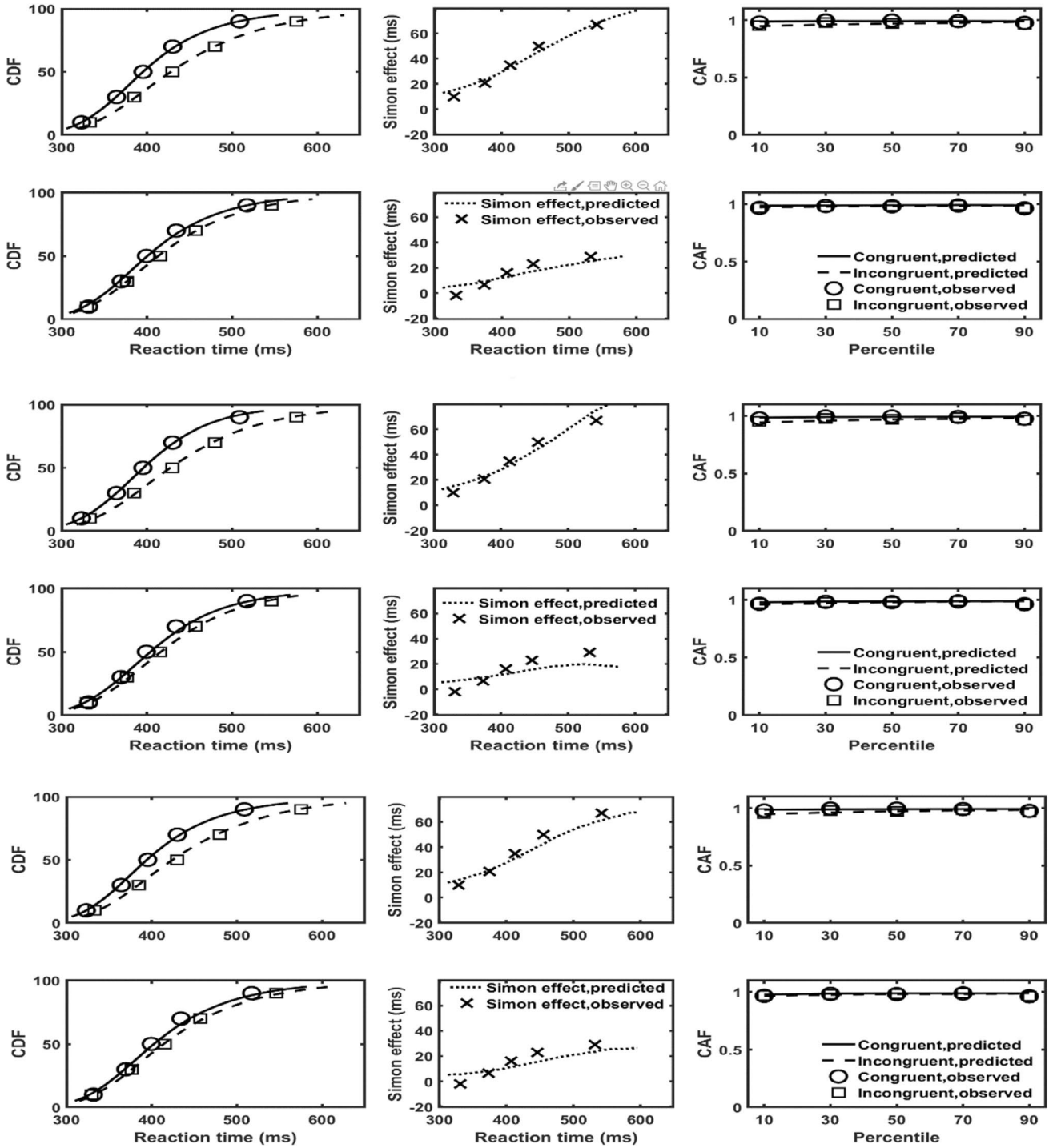

Fig. 2 Conditional duration functions, delta plots and conditional accuracy functions (circles, squares, and crosses) for the CSE in Study 2, together with predictions (solid, dashed, and dotted lines) by the CSE-DMC, FI-DMC and CA-DMC. The first two rows for the CSE-DMC, the third and fourth for the CA-DMC, and the fifth and sixth for the FI-DMC. The first, third, and fifth rows for congruent and congruent trials following congruent trials and the others for congruent and incongruent trials following incongruent trials. *DMC* = diffusion model for conflict tasks, *CSE* = congruency sequence effect

Discussion

On mean RT and accuracy, the arrow-based Simon effect was larger following congruent trials than following incongruent trials, indicating a CSE effect, which replicated previous findings obtained in other conflicting tasks (Funes et al., 2010; Hommel et al., 2004; Kerns, 2006; Stürmer et al., 2002; Yang et al., 2017). The Simon effect on accuracy did not vary with the increase of RT, regardless of whether the prior trial was congruent or incongruent, suggesting that the RT distribution of the Simon effect on accuracy was invariant of the change in RT and not influenced by the preceding trials. Following either a congruent or incongruent trial, the Simon effects on RT increased linearly with the increase of RT. That increase following congruent trials was more rapid than that following incongruent trials, implying that the RT distribution of the Simon effect on the current trials is influenced by the preceding trial. These results together provide evidence that the arrow-based Simon effects on mean RT and RT distribution were influenced by the congruency of the prior trial. Model fitting and comparison showed that the CSE-DMC could fit the CSE well, and the CSE-DMC provided a better fit than the CA-DMC and FI-DMC.

Study 3: RT distributions of CSE and model comparison for Flanker task

For a third evaluation of the CSE-DMC model, we analyzed and modeled the data from Experiment 3 in Luo and Proctor (2016), which used a flanker task in which 26 participants indicated the direction of an arrow presented on the center of a display screen by pressing the C key or M key. Unlike the experiment fit for Study 2, the target arrow was flanked by two other arrows that were of identical or opposite direction compared to the middle arrow. The three arrows were displayed in the same large object or separately in three identical small objects. There were two trial blocks, one for vertical displays for which the arrows were up- or down-pointing and the other for horizontal displays for which the arrows were left- or right-pointing. Each participant performed two blocks of 128 trials.

Luo and Proctor's (2016) Experiment 3 included three variables: display orientation (horizontal vs. vertical), object condition (same, different) and flanker congruency (congruent vs. incongruent). Results showed a flanker congruency effect, but it was not modulated by the other variables and the influence of preceding trials on the flanker effect was not investigated. Other experiments have found that the flanker effect on RT with arrows as target and flankers shows a negative-going delta plot (Pratte, 2021; Ridderinkhof et al., 2005).

In the present study, we first used Vincentile analysis, as in Studies 1 and 2, to analyze the RT distributions for CSE. Then, based on the RT distributions, we fit them with the CSE-DMC to examine whether it can fit the data well and whether the fit is better than that of two other variants, the FI-DMC and the CA-DMC model. This study thus provides evidence as to whether the CSE-DMC can also summarize the results from flanker task and provide a better fit than those of two other variants.

Method

The trial sequences were coded as in Studies 1 and 2 as cC, cI, iC, and iI for congruity or incongruity on prior and current trials. CAFs and CDFs were calculated as in Study 1, and the ANOVAs on them and the model fitting procedure were identical to those in Study 1.

Results

Vincentile analysis on accuracy

The numbers of trials for each trial sequence across participants are shown in Table 1. The main effect of preceding congruency was not significant, $F < 1$, but that of bin was, $F(4, 100) = 4.17$, $p = .004$, $MSE = .003$, $\eta_p^2 = .143$. The main effect of current congruency approached significance, $F(1, 25) = 3.68$, $p = .067$, $MSE = .005$, $\eta_p^2 = .128$. The preceding congruency × current congruency interaction was not significant, $F < 1$, nor were the other interactions, $ps > .365$.

Vincentile analysis on RT

Mean RT and SD per trial sequence across participants are shown in Table 1. The main effect of preceding congruency was not significant, $F < 1$, but those of current congruency and bin were significant, $F(1, 25) = 27.03$, $p < .001$, $MSE = 2{,}622$, $\eta_p^2 = .520$; $F(4, 100) = 192.32$, $p < .001$, $MSE = 2{,}988$, $\eta_p^2 = .885$. Preceding congruency interacted with current congruency, $F(1, 25) = 4.75$, $p = .039$, $MSE = 555$, $\eta_p^2 = .160$, with the flanker effect being larger following congruent trials (27 ms) than following incongruent trials (19 ms).

The two-way interactions of preceding congruency × bin and of current congruency × bin were not significant, $F < 1$; $F(4, 100) = 1.87$, $p = .121$, $MSE = 153$, $\eta_p^2 = .121$, but the three-way interaction of preceding congruency × current congruency × bin was significant, $F(4, 100) = 3.88$, $p = .006$, $MSE = 199$, $\eta_p^2 = .134$. As evident in Fig. 3, when the preceding trial was congruent, trend analysis showed that the flanker effect (cI - cC) did not increase linearly, $F < 1$, but varied quadratically from bin 1 to

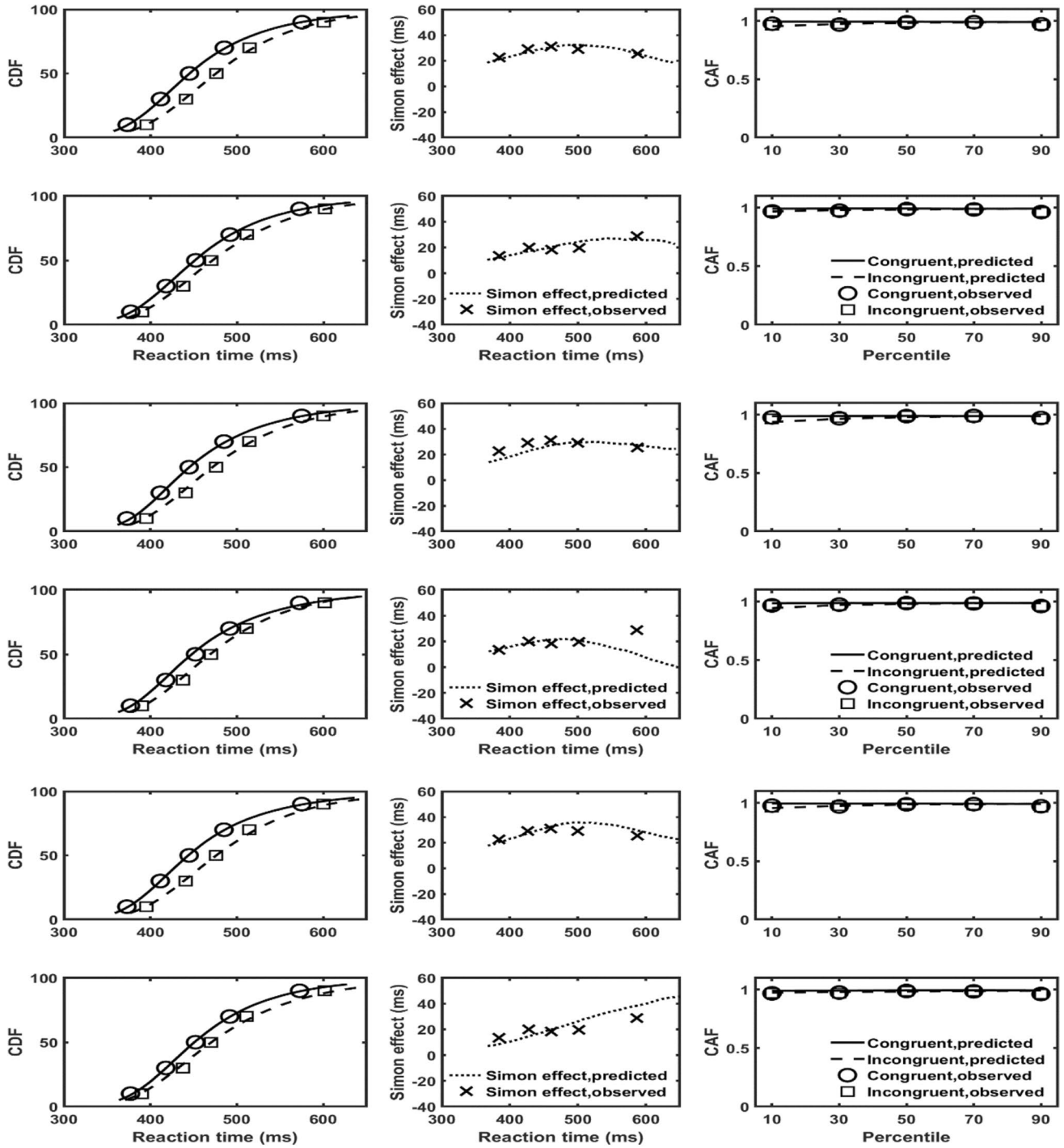

Fig. 3 Conditional duration functions, delta plots and conditional accuracy functions (circles, squares and crosses) for the CSE in Study 3, together with predictions (solid, dashed and dotted lines) by the CSE-DMC, FI-DMC and CA-DMC. The first two rows for the CSE-DMC, the third and fourth for the FI-DMC, and the fifth and sixth for the CA-DMC. The first, third, and fifth rows for congruent and congruent trials following congruent trials and the others for congruent and incongruent trials following incongruent trials. *DMC* = diffusion model for conflict tasks, *CSE* = congruency sequence effect

bin 5 (23, 30, 32, 31, and 22 ms, respectively) $F(1, 25) = 5.40$, $p = .029$, $MSE = 647$, $\eta_p^2 = .178$. However, following an incongruent trial, the flanker effect (iI - iC) increased linearly from bin 1 to bin 5 (13, 19, 15, 16 and 32 ms, respectively), $F(1, 25) = 4.80$, $p = .038$, $MSE = 648$, $\eta_p^2 = .161$, indicating a positive-going delta plot. These results

show that the flanker effects following congruent and incongruent trials had somewhat different RT distributions: the former peaked at the middle bins (2–4), whereas the latter was largest at bin 5.

Model fitting and comparison

The fits of the FI-DMC, CA-DMC and CSE-DMC models were compared using the paired-sample permutation test across 1,000 simulated G^2 and *BIC* values with 100,000 permutations. The FI-DMC and CA-DMC had larger G^2 (54.6 and 51.1) and *BIC* (99.6 and 100.6) values compared with the CSE-DMC ($G^2 = 40.0$; $BIC = 95.0$), $ps < .001$. Results for the CSE together with predictions by the FI-DMC and CA-DMC and CSE-DMC models are shown in Fig. 3. The parameters of the FI-DMC, CA-DMC and CSE-DMC models are shown in Table 2. These results indicate that the CSE-DMC could fit the data well and that it provided a better fit with the data than the other models.

Discussion

On mean RT, the flanker effect was larger following congruent trials than following incongruent trials, indicating a CSE effect, replicating previous findings obtained in flanker and other conflict tasks (Gratton et al., 1992; Wühr & Ansorge, 2005). The flanker effect on accuracy did not vary with the increase of RT, regardless of whether the prior trial was congruent or incongruent, suggesting that the RT distribution of the flanker effect on accuracy was invariant of the change in RT and is not influenced by the preceding trials. Following a congruent trial, the flanker effect on RT increased quadratically with the increase of RT, similar to previous results that delta plot shows an inverted-U shape when targets and flankers are arrows pointing to the left or right (e.g., Pratte, 2021; Ridderinkhof et al., 2005), whereas following an incongruent trial, the flanker effect on RT increased linearly with increasing RT. These results together showed that the flanker effects on mean RT and RT distribution were influenced by the congruency of the prior trial. As with the spatial and arrow-based Simon effects, model fitting and comparison showed that the CSE-DMC could fit the CSE well, and the CSE-DMC provided a better fit than the CA-DMC and FI-DMC.

General discussion

The present study examined the RT distribution of the CSE and extended the DMC to model the RT distribution reflected by delta plots in the spatial- and arrow-based Simon and flanker tasks to understand how the preceding trials influence decision-making on the current trials. Results of Study 1 showed that the Simon effect on accuracy decreased with increasing RT, invariant of following congruent or incongruent trials, showing a negative-going delta plot. On mean RT, following congruent trials, the Simon effect was almost unchanged with the increasing RT, whereas following incongruent trials, the Simon effect became smaller and reversed with the increase of RT, showing a negative-going delta plot. The outcome suggests that the spatial Simon effects following congruent and incongruent trials have different RT distributions, and the reduction of Simon effect on RT with the increasing RT, which usually occurs in the Simon task without investigating the effect of preceding trials, mainly arises from the Simon effect following incongruent trials.

Study 2 showed that, on accuracy, the arrow-based Simon effect following congruent and incongruent trials did not vary with the increasing RT, suggesting that the RT distribution of the effect on accuracy was uninfluenced by the preceding trial type. On RT, following congruent or incongruent trials, the arrow-based Simon effects increased linearly with the increasing RT, with the former showing a more rapid change than the latter, implying that the RT distribution of the Simon effect on the current trials varies with the change of RT and is influenced by the preceding trials.

Results of Study 3 showed that the flanker effect on accuracy did not vary with the increase of RT, regardless of congruency on the prior trial, suggesting the RT distribution of the flanker effect on accuracy invariant of the change in RT and is not influenced by the preceding trials. However, following a congruent trial, the flanker effects on RT increased quadratically with the increase of RT, whereas following an incongruent trial, the flanker effects on RT increased linearly with increasing RT. These results suggested that the RT distribution of the flanker effect on the current trials varies with the change of RT and is influenced by the preceding trials. To our knowledge, few studies have explored the RT distributions of the spatial and arrow-based Simon effects and the flanker effect modulated by preceding trials (CSE) reflected by delta plots, and hence few theories and models have been proposed to explain how CSEs vary with the increasing RT.

In Studies 1–3, we also found the CSE on mean RT with a larger spatial, arrow-based Simon, or flanker effect following congruent trials than that following incongruent trials; a similar pattern of results also emerged on mean accuracy in Studies 1 and 2. The disparities of Simon and flanker effects on mean RT following congruent and incongruent trials are most often explained with the conflict adaptation accounts (Botvinick et al., 2001; Gratton et al., 1992; see also Verguts & Notebaert, 2008, 2009),

for which there are at least two versions that make somewhat different assumptions. Their identical claims are that in conflict tasks, on incongruent trials, attention to the task-irrelevant attributes or flankers can be reduced, as it can impede responses, resulting in a smaller interference with performance on the upcoming trial. In contrast, on congruent trials, attention to the task-irrelevant attributes or flankers can be sustained or increased, as this can help the processing of stimulus, resulting in larger interference with performance on the upcoming trial.

The conflict adaptation account can explain the spatial and arrow-based Simon and flanker effects on mean RT and the former two effects on mean accuracy, but it does not seem to offer an explanation of the different RT distributions for the conflict effects following congruent and incongruent trials. Specifically, according to this account, the conflict effect following congruent trials should increase with increasing RT, whereas that following incongruent trials should decrease. On congruent trials, attention to the task-irrelevant attributes can be sustained or increased with the increasing RT, as it can help the processing of task-irrelevant attributes. When such allocation of attention transfers to the upcoming trials, it likely speeds up responses on congruent trials and slows responses on incongruent trials, resulting in the conflict effect increasing gradually on the upcoming trial. By contrast, on incongruent trials, attention to the task-irrelevant attributes should be reduced with increasing RT, as it can interfere with the processing of task-relevant attributes. When such allocation of attention transfers to the next trial, it likely slows down the responses on congruent trials and speeds up the responses on incongruent trials, resulting in the conflict effect decreasing gradually on that trial. Therefore, the conflict adaptation account can explain that the arrow-based Simon effect following congruent trials increased with increasing RT but not that the spatial Simon effect almost did not vary and the flanker effect changed quadratically. The conflict adaptation account also can explain the decrease of the spatial Simon effect across the RT distribution following incongruent trials, or even its reversal, but it cannot explain the increase of the arrow-based Simon and flanker effects with the increase of RT.

The feature-integration account (Hommel et al., 2004; Mayr et al., 2003) assumes that stimulus and response features are coded and integrated within a common, transient "event file." Consequently, each trial likely leaves behind a binding of particular stimulus and response features from the preceding trial that can overlap partially or wholly with the stimulus and response features on the current trial. For cC or iI trial sequences, complete match or mismatch occurs as the stimulus location and response position on the preceding trial can both repeat or both change on the current trial, which speeds up responses. For cI and iC trial sequences, partial repetition occurs as the stimulus location and response position repeats on the current trial but not both, which likely results in a stimulus-response binding conflict and slows down the responses (Erb et al., 2016; Hommel, 2004). This account could explain why the spatial and arrow-based Simon effects on mean RT and accuracy, and the larger flanker effect on mean RT, are larger following congruent trials than following incongruent trials. As the event files are transient, their effect likely sustains for a short time (Hommel & Frings, 2020), so the feature integration account can explain that the spatial Simon effect following incongruent trials becomes smaller with increasing RT, but not that the effect reversed for those slower responses and that the effect following congruent trials was almost unchanged with increasing RT. This account also cannot easily explain that the arrow-based Simon effects following congruent and incongruent trials increased with the increasing RT, and the former changed more rapidly, or why the flanker effects on RT increased quadratically with the increase of RT following congruent trials but linearly following incongruent trials.

Overall, the conflict adaptation and feature integration accounts have seldom been used to explain the RT distributions of CSE, and more assumptions are needed to account for these results. Consequently, we extended the DMC to explain these results, given that the DMC has provided a complete account of the RT distributions of Simon effect including the congruent and incongruent conditions (Evans & Servant, 2020; Luo & Proctor, 2019; Ulrich et al., 2015; White et al., 2018).

The CSE-DMC we proposed inherits the assumptions of the DMC that the controlled processes accumulate linearly but the automatic processes vary with the increasing RT. Another two assumptions were added to the expanded model. The first is that feature integration influences only the controlled processes. As whole repetition/switch of trial type likely speeds up the responses for cC and iI trial sequences and partial repetition likely slows down the responses for cI and iC trial sequences, the drift rate for the controlled processes for cC and iI trial sequences is smaller than that for iC and cI trial sequences. The second assumption is that following incongruent trials, the automatic processes are influenced, resulting in more attention paid to the target and reduction of influence of the distractor. Accordingly, for iC and iI trial sequences, the drift rate for the automatic processes becomes smaller. Therefore, the CSE-DMC is developed from the DMC and is inspired by the assumptions from the feature-integration account and the conflict adaption accounts.

According to the CSE-DMC, except for the drift rates, b and the other parameters are identical across trial sequences, so the RT and accuracy for each trial sequence are determined by their corresponding drift rate. Consequently, the Simon effect following congruent trials is determined by

the difference between $\mu_{cC}(t)$ and $\mu_{cI}(t)$, whereas the Simon effect following incongruent trials is determined by the difference between $\mu_{iC}(t)$ and $\mu_{iI}(t)$. As $\mu_{cC}(t)$ minus $\mu_{cI}(t)$ equals μ_{cL} - $\mu_c + 2\mu_a(t)$, which is larger than $\mu_{iC}(t)$ minus $\mu_{iI}(t)$ that equals μ_c - $\mu_{cL} + 2\mu_{aS}(t)$, it results in a larger Simon effect following congruent trials than following incongruent trials. Moreover, for the CSE-DMC, $\mu_{cI}(t) < \mu_{iC}(t) < \mu_{cC}(t)$ and $\mu_{cI}(t) < \mu_{iI}(t) < \mu_{cC}(t)$, and $\mu_{iI}(t)$ minus $\mu_{iC}(t)$ equals μ_{cL} - μ_c - $2\mu_{aS}(t)$, which determines the difference between $\mu_{iI}(t)$ and $\mu_{iC}(t)$. According to function (1), with the threshold and other parameters being constant across trial sequences, the size of drift rate for each trial sequence determines the speeds of decision-making related to tradeoff between response speed and accuracy, with high drift rates resulting in faster and more accurate decisions (Pedersen et al., 2017). Consequently, for cI and cC, the slowest and fastest decisions are made, respectively, and for iC and iI, the speeds of decisions are located at between cI and cC, and the differences between iC and iI are determined by task situations. Model fitting and comparison showed that the CSE-DMC could fit better with the RT distributions reflected by delta plot than the other variants, the FI-DMC and the CA-DMC models. This outcome provides evidence that preceding trials can influence the decisions on the current trials by using different modes to modulate the automatic processing and controlled processes.

According to the DMC, the shape of the delta plot is determined by automatic processes by changing the parameter τ, as the drift rates for the controlled processes are identical for congruent and incongruent conditions. For the CSE-DMC, as the drift rates for the controlled processes are not identical across trial sequences, the shape of delta plot is influenced by both automatic and controlled processes. For trial sequences cC and cI, their drift rates for automatic processes are $\mu_a(t)$ and the drift rates for the controlled processes are μ_{cL} and μ_c, respectively. For trial sequence cC, if the response on current trial is not influenced by that on preceding trial, $\mu_{cC}(t)$ is equal to μ_c plus $\mu_a(t)$. As $\mu_{cC}(t)$ is larger than μ_c plus $\mu_a(t)$, it speeds up equivalently the responses for trial sequence cC, which likely increases (decreases) temporal overlap of codes of color and stimulus location (direction of arrow), as stimulus location (direction of arrow) is processed faster (slower) than color. Such changes of temporal overlap likely make the spatial Simon effect not reduced and arrow-based Simon effect increases rapidly with increasing RT, because temporal overlap manipulations of codes of task-relevant and task-irrelevant attributes can influence the magnitude and time course of the conflict effect (Hübner & Töbel., 2019; Miles & Proctor., 2009; Pratte, 2021).

For trial sequences iC and iI, the drift rates for the controlled processes are μ_c and μ_{cL} and the drift rates for automatic processes are reduced as $\mu_{aS}(t)$. This reduction likely makes the spatial Simon effect reduce slowly and arrow-based Simon effect increase slowly. Likewise, for trial sequence iI, if the response on current trial is not influenced by that on preceding trial, $\mu_{iI}(t)$ is equal to μ_c minus $\mu_{aS}(t)$. As $\mu_{iI}(t)$ is larger than μ_c minus $\mu_{aS}(t)$, it speeds up equivalently the responses for trial sequence iI, which likely decreases temporal overlap of codes of target and flanking arrows. Such changes of temporal overlap likely make the flanker effect occurs lately, resulting in a positive going delta plot.

Recently, Schuch and Pütz (2021) used the standard diffusion model and task-switching paradigm with parity (odd/even) and magnitude (smaller/larger than five) tasks to explore the affective modulation of conflict adaptation (the difference between the congruency effects following congruent and incongruent trial). Results showed that the conflict adaptation on drift rates or of thresholds following congruent trials was larger than that following incongruent trials, suggesting that response conflict on previous trial increases processing speed and response caution. The findings of Schuch and Pütz are compatible with those of Erb and colleagues (Erb et al., 2016, 2019; Erb & Marcovitch, 2018, 2019) with a reach-tracking technique to link the spatial and temporal characteristics of hand movements to the dynamics of cognitive control. Across the Stroop (1935), Eriksen flanker (Eriksen & Eriksen, 1974), and spatial Simon tasks, Erb et al. found significant main effects of previous congruency and current congruency on initiation times, with the pattern of effects: cC < iC < cI < iI. This outcome was consistent with the claim by Erb et al. (2016, 2019) that initiation times can be used to target the functioning of the threshold adjustment process, which indexes how long the "brake" is put on behavior. Conversely, a different pattern of results was obtained on reach curvatures, besides main effects of current congruency and previous congruency, an interaction between them was obtained, with larger congruency effect following congruent trials than following incongruent trials. Erb et al. (2016, 2019) hence proposed that reach curvatures could be used to target the functioning of the controlled selection process, by indexing the degree of coactivation between competing responses over the course of a trial. However, these claims were made by speculations based on experimental results, and further research can test them directly by fitting the data with the standard diffusion model.

The disparities of the CSE-DMC and these findings are that the model assumes that trial sequence influences the drift rates including automatic and controlled processing components but not the threshold. However, Schuch and Pütz (2021) used the standard diffusion model and concluded that the drift rate and threshold were influenced by trial sequence. Given that the standard diffusion model cannot simulate the negative-going delta plot for the spatial Simon effect (Ulrich et al., 2015), further research needs to

test whether both the threshold and drift rate for controlled process in the CSE-DMC are influenced by trial sequence or whether only the latter is. Further research also needs to test another possibility that overall threshold for gating, controlled processes, and automatic processes are involved in the CSE, as neurocomputational model has suggested that the three routes might be involved in the conflict resolution of congruency effect (Wiecki & Frank, 2013).

A limitation of the present research is that it relied on existing data sets. For the assumption that feature integration only influences the controlled processes, we used only one parameter μ_{cL} for the controlled processes for cC and iI trial sequences. As indicated, this is because complete repetition or switch of trial type speeds up the responses for cC and iI trial sequences, although to different extents. Moreover, as our main aim was not to test the feature integration and conflict adaptation accounts, we have not evaluated whether excluding complete repetition trials from analysis impacts the results on mean RTs and accuracies. Because the datasets were not collected with that purpose in mind, excluding complete repetition trials from analysis in the current study does not provide enough cC and iI trial sequences to perform RT distribution analyses of CSE and model fitting. However, using only one parameter μ_{cL} for the controlled processes for cC and iI trial sequences includes an implicit assumption that there are similar RT distributions for complete repetition or switch of trial type within cC and iI trial sequences. Additional research is needed that is designed specifically to examine whether there are similar RT distributions for complete repetition and switch of trial type (mismatch trials), and whether excluding complete repetition trials from analysis impacts the results on mean RTs, accuracies and RT distribution. Doing so can test the feature integration account (Hommel, 2004) and help understand how feature integration influences the controlled processes.

In Study 1, following incongruent trials, the predicted delta function undershot the x-axis, which apparently arises from a small numerical error due to use of the Euler method. The problem might be solved with high performance computing if the step size converges toward zero. However, it should be noted that the present CSE-DMC cannot predict the reverse Simon effect occurring at long RTs, because on these trials the effect of automatic processes cannot become a facilitatory effect on the response. Therefore, to explain the reverse Simon effect occurring at long RTs, if it is not a numerical error, an executive control process is required to include in the dual-process concept model, which selectively suppresses the automatically activated processes (De Jong et al., 1994; Hübner & Töbel, 2019; Ridderinkhof, 2002). Future research needs to examine the conditions for which the CSE-DMC predicts an advantage for incongruent trials at long RTs, and whether inclusion of a specific inhibitory process is necessary to explain such results.

In conclusion, the spatial and arrow-based Simon, and flanker effects following congruent and incongruent trials are different on mean RT and on the level of RT distributions reflected by delta plots. These disparities of mean RTs and RT distributions for these trial sequences could be a consequence of the automatic and controlled processes of conflict stimulus activation on the current trial being influenced differently by the prior trial. We provided evidence for this supposition by showing that the hypothesized computational mechanisms underlying these processes can be instantiated within the CSE-DMC.

Funding This research was supported by grants from the National Science Foundation of China (31470984, 62061136001) and National Social Science Foundation of China (20&ZD296).

Declarations

Conflict of interest The authors have declared that no competing interests exist.

References

Abrahamse, E., Braem, S., Notebaert, W., & Verguts, T. (2016). Grounding cognitive control in associative learning. *Psychological Bulletin, 142*, 693–728.

Bausenhart, K. M., Ulrich, R., & Miller, J. (2021). Effects of conflict trial proportion: A comparison of the Eriksen and Simon tasks. *Attention, Perception & Psychophysics, 83*, 810–836.

Botvinick, M. M., Braver, T. S., Barch, D. M., Carter, C. S., & Cohen, J. D. (2001). Conflict monitoring and cognitive control. *Psychological Review, 108*(3), 624–652.

Cespón, J., Hommel, B., Korsch, M., & Galashan, D. (2020). The neurocognitive underpinnings of the Simon effect: An integrative review of current research. *Cognitive, Affective, and Behavioral Neuroscience, 20*, 1133–1172.

De Jong, R., Liang, C.-C., & Lauber, E. (1994). Conditional and unconditional automaticity: A dual-process model of effects of spatial stimulus-response correspondence. *Journal of Experimental Psychology: Human Perception and Performance, 20*, 731–750.

De Pisapia, N., & Braver, T. S. (2006). A model of dual control mechanisms through anterior cingulate and prefrontal cortex interactions. *Neurocomputing, 69*, 1322–1326.

Egner, T., & Hirsch, J. (2005). Cognitive control mechanisms resolve conflict through cortical amplification of task-relevant information. *Nature Neuroscience, 8*, 1784–1790.

Erb, C. D., & Marcovitch, S. (2018). Deconstructing the Gratton effect: Targeting dissociable trial sequence effects in children, pre-adolescents, and adults. *Cognition, 179*, 150–162.

Erb, C. D., & Marcovitch, S. (2019). Tracking the within-trial, cross-trial, and developmental dynamics of cognitive control: Evidence from the Simon task. *Child Development, 90*, e831–e848.

Erb, C. D., McBride, A., & Marcovitch, S. (2019). Associative priming and conflict differentially affect two processes underlying cognitive control: Evidence from reaching behavior. *Psychonomic Bulletin & Review, 26*, 1400–1410.

Erb, C. D., Moher, J., Sobel, D. M., & Song, J. (2016). Reach tracking reveals dissociable processes underlying cognitive control. *Cognition, 152*, 114–126.

Eriksen, B. A., & Eriksen, C. W. (1974). Effects of noise letters upon the identification of a target letter in a nonsearch task. *Perception & Psychophysics, 16*, 143–149.

Evans, N. J., & Servant, M. (2020). A comparison of conflict diffusion models in the flanker task through pseudolikelihood Bayes factors. *Psychological Review, 127*, 114–135.

Frank, M. J. (2006). Hold your horses: A dynamic computational role for the subthalamic nucleus in decision making. *Neural Networks, 19*, 1120–1136.

Funes, M. J., Lupiáñez, J., & Humphreys, G. (2010). Analyzing the generality of conflict adaptation effects. *Journal of Experimental Psychology. Human Perception and Performance, 36*, 147–161.

Gratton, G., Coles, M. G. H., & Donchin, E. (1992). Optimizing the use of information: Strategic control of activation of responses. *Journal of Experimental Psychology: General, 121*, 480–506.

Hommel, B. (1994). Spontaneous decay of response-code activation. *Psychological Research, 56*, 261–268.

Hommel, B. (2004). Event files: feature binding in and across perception and action. *Trends in Cognitive Sciences, 8,* 494–500.

Hommel, B. (2022). GOALIATH: A theory of goal-directed behavior. *Psychological Research, 86*, 1054–1077.

Hommel, B., & Frings, C. (2020). The disintegration of event files over time: Decay or interference? *Psychonomic Bulletin & Review, 27*(4), 751–757.

Hommel, B., Proctor, R. W., & Vu, K. P. (2004). A feature-integration account of sequential effects in the Simon task. *Psychological Research, 68*(1), 1–17.

Hübner, R. (2014). Does attentional selectivity in global/local processing improve discretely or gradually? *Frontiers in Psychology, 5*, 61.

Hübner, R., Steinhauser, M., & Lehle, C. (2010). A dual-stage two-phase model of selective attention. *Psychological Review, 117*, 759–784.

Hübner, R., & Töbel, L. (2019). Conflict resolution in the Eriksen flanker task: Similarities and differences to the Simon task. *PLoS ONE, 14*, e0214203.

Janczyk, M., & Lerche, V. (2019). A diffusion model analysis of the response-effect compatibility effect. *Journal of Experimental Psychology: General, 148*, 237–251.

Kerns, J. G. (2006). Anterior cingulate and prefrontal cortex activity in an FMRI study of trial-to-trial adjustments on the Simon task. *NeuroImage, 33*(1), 399–405.

Kim, S., & Cho, Y. S. (2014). Congruency sequence effect without feature integration and contingency learning. *Acta Psychologica, 149*, 60–68.

Kalanthroff, E., Davelaar, E. J., Henik, A., Goldfarb, L., & Usher, M. (2018). Task conflict and proactive control: A computational theory of the Stroop task. *Psychological Review, 125*, 59–82.

Lagarias, J. C., Reeds, J. A., Wright, M. H., & Wright, P. E. (1998). Convergence properties of the Nelder–Mead simplex method in low dimensions. SIAM *Journal on Optimization, 9*, 112–147.

Lim, C. E., & Cho, Y. S. (2021). Response mode modulates the congruency sequence effect in spatial conflict tasks: Evidence from aimed-movement responses. *Psychological Research, 85*, 2047–2068.

Luo, C., & Proctor, R. W. (2017). How different location modes influence responses in a Simon-like task. *Psychological Research, 81*, 1125–1134.

Luo, C., & Proctor, R. W. (2018). The location-, word- and arrow-based Simon effects: An ex-Gaussian analysis. *Memory & Cognition, 46*, 497–506.

Luo, C., & Proctor, R. W. (2019). How different direct association routes influence the indirect route in the same Simon-like task. *Psychological Research, 83*, 1733–1748.

Luo, C., & Proctor, R. W. (2020a). Shared mechanisms underlying the location-, word- and arrow-based Simon effects. *Psychological Research, 84*, 1655–1667.

Luo, C., & Proctor, R. W. (2020b). The location-based Simon effect: Reliability of ex-Gaussian analysis. *Memory & Cognition, 48*, 42–50.

Luo, C., & Proctor, R. W. (2021). Word- and arrow-based Simon effects emerge for eccentrically presented location words and arrows. *Psychological Research, 85*, 816–827.

Mackenzie, I. G., & Dudschig, C. (2021). DMCfun: An R package for fitting Diffusion Model of Conflict (DMC) to reaction time and error rate data. *Methods in Psychology, 5*, 100074.

Mahani, M.-A. N., Bausenhart, K. M., Ahmadabadi, M. N., & Ulrich, R. (2019). Multimodal Simon effect: A multimodal extension of the diffusion model for conflict tasks. *Frontiers in Human Neuroscience., 12*, 507.

Mayr, U., Awh, E., & Laurey, P. (2003). Conflict adaptation effects in the absence of executive control. *Nature Neuroscience, 6*, 450–452.

Metropolis, N., & Ulam, S. (1949). The Monte Carlo method. *Journal of the American Statistical Association, 44*, 335–341.

O'Connell, R. G., Shadlen, M. N., Wong-Lin, K., & Kelly, S. P. (2018). Bridging neural and computational viewpoints on perceptual decision-making. *Trends in Neurosciences, 11*, 838–852.

Pedersen, M. L., Frank, M. J., & Biele, G. (2017). The drift diffusion model as the choice rule in reinforcement learning. *Psychonomic Bulletin & Review, 24*, 1234–1251.

Pratte, M. S. (2021). Eriksen flanker delta plot shapes depend on the stimulus. *Attention, Perception & Psychophysics, 83*, 685–699.

Proctor, R. W., Miles, J. D., & Baroni, G. (2011). Reaction time distribution analysis of spatial correspondence effects. *Psychonomic Bulletin & Review, 18*, 242–266.

Ratcliff, R. (1979). Group reaction time distributions and an analysis of distribution statistics. *Psychological Bulletin, 86*, 446–461.

Ratcliff, R., & McKoon, G. (2020). Decision making in numeracy tasks with spatially continuous scales. *Cognitive Psychology, 116*, 101259.

Ratcliff, R., & Smith, P. L. (2004). A comparison of sequential sampling models for two-choice reaction time. *Psychological Review, 111*, 333–367.

Ratcliff, R., Smith, P. L., Brown, S. D., & McKoon, G. (2016). Diffusion Decision Model: Current Issues and History. *Trends in Cognitive Sciences, 20*, 260–281.

Ridderinkhof, K. R. (2002). Activation and suppression in conflict tasks: Empirical clarification through distributional analyses. In W. Prinz & B. Hommel (Eds.), *Common mechanisms in perception and action: Attention and performance XIX* (pp. 494–519). Oxford University Press.

Ridderinkhof, K. R., Scheres, A., Oosterlaan, J., & Sergeant, J. A. (2005). Delta plots in the study of individual differences: New tools reveal response inhibition deficits in AD/HD that are eliminated by methylphenidate treatment. *Journal of Abnormal Psychology, 114*, 197–215.

Spapé, M. M., Band, G. P. H., & Hommel, B. (2011). Compatibility sequence effects in the Simon task reflect episodic retrieval but not conflict adaptation: Evidence from LRP and N2. *Biological Psychology, 88*, 116–123.

Schmidt, J. R. (2013). Questioning conflict adaptation: Proportion congruent and Gratton effects reconsidered. *Psychonomic Bulletin & Review, 20*, 615–630.

Schmidt, J. R. (2019). Evidence against conflict monitoring and adaptation: An updated review. *Psychonomic Bulletin & Review, 26*, 753–771.

Schuch, S., & Pütz, S. (2021). Mood state and conflict adaptation: An update and a diffusion model analysis. *Psychological Research, 85*, 322–344.

Schwarz, W., & Miller, J. (2012). Response time models of delta plots with negative-going slopes. *Psychonomic Bulletin and Review, 19*, 555–574.

Servant, M., White, C., Montagnini, A., & Burle, B. (2015). Using covert response activation to test latent assumptions of formal decision-making models in humans. *Journal of Neuroscience, 35*, 10371–10385.

Servant, M., White, C., Montagnini, A., & Burle, B. (2016). Linking theoretical decision-making mechanisms in the Simon task with electrophysiological data: A model-based neuroscience study in humans. *Journal of Cognitive Neuroscience, 28*, 1501–1521.

Shenhav, A., Botvinick, M. M., & Cohen, J. D. (2013). The expected value of control: An integrative theory of anterior cingulate cortex function. *Neuron, 79*, 217–240.

Simon, J. R. (1969). Reactions toward the source of stimulation. *Journal of Experimental Psychology, 81*, 174–176.

Stroop, J. R. (1935/1992). Studies of interference in serial verbal reactions. *Journal of Experimental Psychology, 18*, 643–662. [reprinted in Journal of Experimental Psychology: General, 121, 15–23]

Stürmer, B., Leuthold, H., Soetens, E., Schröter, H., & Sommer, W. (2002). Control over location-based response activation in the Simon task: Behavioral and electrophysiological evidence. *Journal of Experimental Psychology: Human Perception and Performance, 28*, 1345–1363.

Töbel, L., Hübner, R., & Stürmer, B. (2014). Suppression of irrelevant activation in the horizontal and vertical Simon task differs quantitatively not qualitatively. *Acta Psychologica, 152*, 47–55.

Ulrich, R., Schröter, H., Leuthold, H., & Birngruber, T. (2015). Automatic and controlled stimulus processing in conflict tasks: superimposed diffusion processes and delta functions. *Cognitive Psychology, 78*, 148–174.

Verguts, T., & Notebaert, W. (2008). Hebbian learning of cognitive control: Dealing with specific and nonspecific adaptation. *Psychological Review, 115*, 518–525.

Verguts, T., & Notebaert, W. (2009). Adaptation by binding: A learning account of cognitive control. *Trends in Cognitive Sciences, 13*, 252–257.

Weissman, D. H., Jiang, J., & Egner, T. (2014). Determinants of congruency sequence effects without learning and memory confounds. *Journal of Experimental Psychology: Human Perception and Performance, 40*, 2022–2037.

White, C. N., Ratcliff, R., & Starns, J. J. (2011). Diffusion models of the flanker task: Discrete versus gradual attentional selection. *Cognitive Psychology, 63*, 210–238.

White, C. N., Servant, M., & Logan, G. D. (2018). Testing the validity of conflict drift-diffusion models for use in estimating cognitive processes: A parameter-recovery study. *Psychonomic Bulletin & Review, 25*, 286–301.

Wiecki, T. V., & Frank, M. J. (2013). A computational model of inhibitory control in frontal cortex and basal ganglia. *Psychological Review, 120*, 329–355.

Wühr, P., & Ansorge, U. (2005). Exploring trial-by-trial modulations of the Simon effect. *Quarterly Journal of Experimental Psychology, 58A*, 705–731.

Yamaguchi, M., & Proctor, R. W. (2012). Multidimensional vector model of stimulus–response compatibility. *Psychological Review, 119*, 272–303.

Yang, G., Nan, W., Zheng, Y., Wu, H., Li, Q., & Liu, X. (2017). Distinct cognitive control mechanisms as revealed by modality-specific conflict adaptation effects. *Journal of Experimental Psychology: Human Perception and Performance, 43*(4), 807–818.

Publisher's note Springer Nature remains neutral with regard to jurisdictional claims in published maps and institutional affiliations.